



Contents lists available at ScienceDirect

## Quaternary Research

journal homepage: [www.elsevier.com/locate/yqres](http://www.elsevier.com/locate/yqres)

## Short Paper

## Sedimentary evolution of a late Pleistocene wetland indicating extreme coastal uplift in southern Tanzania

Markus Reuter<sup>a,\*</sup>, W.E. Piller<sup>a</sup>, M. Harzhauser<sup>b</sup>, B. Berning<sup>c</sup>, A. Kroh<sup>b</sup><sup>a</sup> Institute for Earth Sciences, Graz University, Heinrichstr. 26, A-8010 Graz, Austria<sup>b</sup> Natural History Museum Vienna, Burgring 7, A-1010 Vienna, Austria<sup>c</sup> Upper Austrian State Museum, Welsstr. 20, A-4060 Linz-Leonding, Austria

## ARTICLE INFO

## Article history:

Received 1 December 2008

Available online xxxx

## Keywords:

Coastal terrace

Facies

Sea level

Neotectonics

Weichselian

Tanzania

## ABSTRACT

Facies analyses of Pleistocene deposits from southern coastal Tanzania (Lindi District) document that sediments formed in a wetland evolving on a coastal terrace in the Lindi Fracture Zone foreland. The exposed succession shows a marked sedimentary change from tidal to terrestrial facies. <sup>14</sup>C analyses on gastropod shells indicate the emergence of the Lindi coast at ~44 <sup>14</sup>C ka BP. Emergence and subsequent elevation of terraces to 21 m above present-day sea level was linked to the falling eustatic sea level prior to the last glacial maximum, and to a periodic elevation due to extensional tectonic episodes in the eastern branch of the East African Rift System (EARS). Since ~44 <sup>14</sup>C ka BP tectonic uplift at the coast was 80–110 m, comparable to that in the extreme uplift areas of the EARS.

© 2009 University of Washington. Published by Elsevier Inc. All rights reserved.

## Introduction

Coastal terraces are important geomorphological features in mainland Tanzania and tectonic uplift is considered the dominant process for their origin (Alexander, 1968; Kent et al., 1971; Schlüter, 1997; Shaghude and Wannäs, 2000; Arthurton, 2003). Nicholas et al. (2007) proposed that Quaternary uplift of coastal terraces correlates with extensional episodes in the eastern arm of the East African Rift System (EARS). Knowledge on the age of coastal terraces provides insight on the frequency, intensity and duration of rifting episodes, and contributes to studies on the regional uplift history at the East African coast and the EARS. Little is known about Quaternary uplift in the East African Rift; especially, its timing is not well-constrained. For the EARS eastern branch major changes from lacustrine to fluvial sedimentation at ~700 ka are reported in the Lake Manyara region (northern Tanzania), which may be related to southward shift of major rift faulting (Ring et al., 2005). There is also little information on the geology of coastal terraces (Braithwaite, 1984; Schlüter, 1997; Arthurton et al., 1999). Alexander (1968) noticed that most recent terrace features in northern coastal Tanzania have been deformed. Late Quaternary tectonism is also indicated for the Kilwa Platform in southern Tanzania. There, Nicholas et al. (2007) proposed a post-Eemian ( $\leq 80$  ka) uplift based on the affinities of benthic foraminiferal faunas from a coral patch reef and beach rock to foraminiferal faunas

from Eemian beach deposits at the eastern coast of South Africa. However, all identified foraminifers (*Ammonia* sp., *Amphistegina* sp., *Challengerella persica*, *Elphidium crispum*, *Operculina* sp., and miliolid species) are typical shallow marine, without biostratigraphic constraints. The poor biostratigraphic control available for the shallow marine and terrestrial settings that developed on coastal platforms and the few outcrops along the coast is a major problem in determining the timing of coastal uplift in Tanzania. Therefore, the elevations of coastal terraces above present-day sea level have been commonly used for correlative stratigraphy in northern Tanzania (Alexander, 1968). However, as outlined by Schlüter (1997), this terrace stratigraphy is controversial and altitude correlation should be treated with caution.

In this paper we combine facies analyses of Pleistocene deposits from southern coastal Tanzania (Lindi District) with AMS <sup>14</sup>C analyses of two samples of fossil gastropod shells to date the emergence of the coast and investigate on the neotectonic uplift.

## Geological setting

The studied outcrop is situated at the southern Tanzanian coast <1 km south of Mbanja village (Fig. 1). It is a quarry at the road between Lindi and Mchinga that was temporarily active for road-works in summer 2007. This outcrop is exceptional for the Tanzanian coast because it is laterally continuous for ~300 m and the recently exposed sediments were still unaffected by vegetation and weathering. The exposed sedimentary succession is totally ~12 m thick. Thickness decreases from ~12 m in the west to ~6 m in the east due to advanced mining. Beds dip ~10° eastward.

\* Corresponding author. Fax: +43 316 3809871.

E-mail addresses: [markus.reuter@uni-graz.at](mailto:markus.reuter@uni-graz.at) (M. Reuter), [werner.piller@uni-graz.at](mailto:werner.piller@uni-graz.at) (W.E. Piller), [mathias.harzhauser@nhm-wien.ac.at](mailto:mathias.harzhauser@nhm-wien.ac.at) (M. Harzhauser), [b.berning@landesmuseum.at](mailto:b.berning@landesmuseum.at) (B. Berning), [andreas.kroh@nhm-wien.ac.at](mailto:andreas.kroh@nhm-wien.ac.at) (A. Kroh).

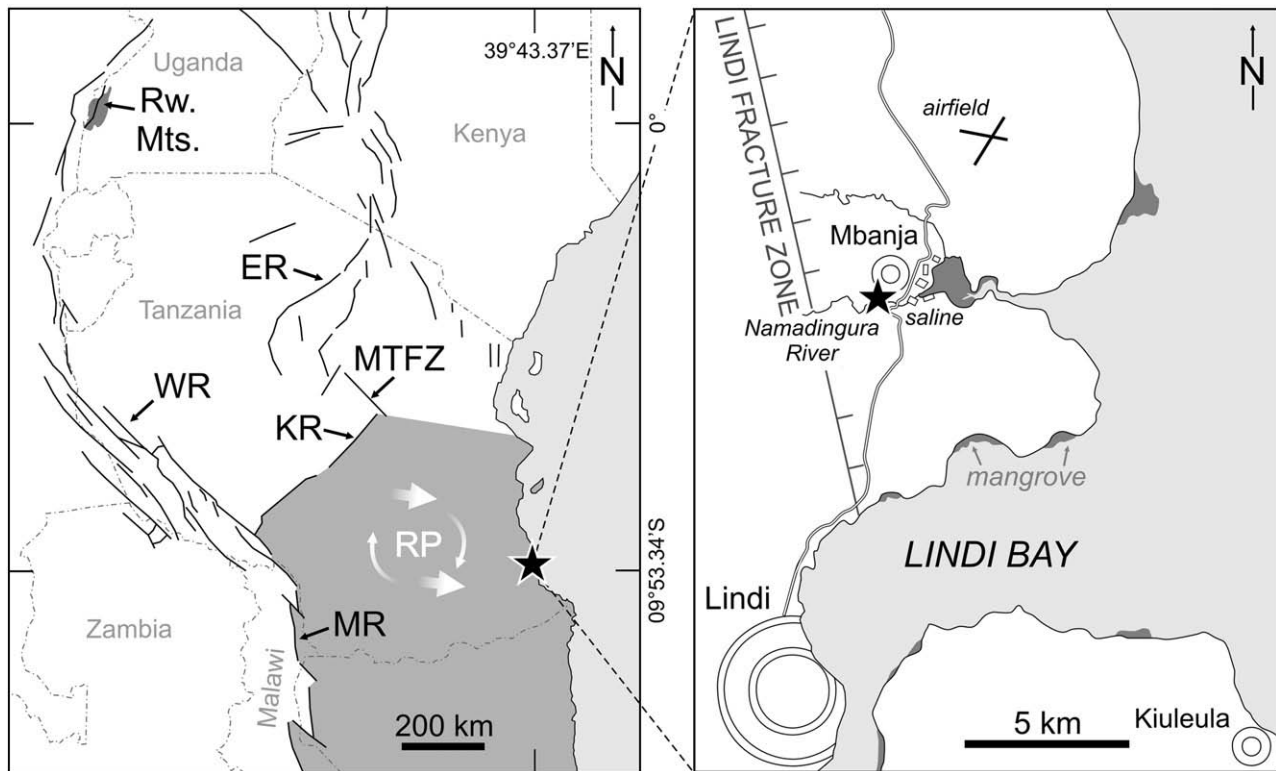


**Figure 1.** Location map and spatial distribution of Cenozoic rifts in Tanzania and adjacent regions (modified after Le Gall et al., 2004; Nicholas et al., 2007; Stamps et al., 2008); ER: Eastern Rift, WR: Western Rift, MR: Malawi Rift, KR: Kilombero Rift, MTFZ: Maminzi Transverse Fault Zone, Rw. Mts.: Rwenzori Mountains; arrows indicate the movement of the Rovuma Microplate (RP), stars mark the position of the studied outcrop at 09°53.34'S, 39°43.37'E.

The sediments were deposited on a coastal terrace that extends between Lindi Bay and Mchinga Bay, located east of the north-north-west orientated Lindi Fracture Zone (LFZ, Fig. 1). In the western part of the outcrop, a north-south striking reverse fault with a vertical offset of ~3 m was observed in the studied sedimentary succession, which is related to the LFZ.

The LFZ developed during the Permian as a result of the rifting of Madagascar away from East Africa due to the break-up of East- and West-Gondwana along the East African coast (Rabinowitz et al., 1983; Nicholas et al., 2007). Since the Oligocene, structural development of coastal Tanzania is linked to the opening of the eastern branch of the EARS in the far north of the country (Forster et al., 1997; Fig. 1). Since the Early Pliocene the southern coast of Tanzania became part of the Rovuma Microplate located south of the EARS eastern branch. During the Quaternary, rifting in the eastern rift branch propagated to the south and moved the Rovuma Microplate east-southeast with a slight clockwise rotation as a consequence of periodic stretching in the EARS eastern branch (Le Gall et al., 2004; Calais et al., 2006; Fig. 1). Nicholas et al. (2007) argue that as a result, the Rovuma Microplate sheared the southern coast of Tanzania against the thickened crust of the comparatively stationary Davie Ridge, which is situated offshore the East African coast and outside the Rovuma Microplate (Mougenot et al., 1986). These transpressive movements reactivated old (Mesozoic and Cenozoic) faults, for instance the LFZ, and induced the uplift of coastal terraces all along the Tanzanian coast (Nicholas et al., 2007).

### Terrace deposits

Mbanja section comprises three depositional units (Fig. 2). Unit 1 is a 2 m thick deposit of calcareous clay. At the top of this unit an oyster (*Ostreidae*) shell-bed occurs (subunit 1a). Unit 2 is a distinct, intensively rooted horizon. In the eastern part of the outcrop calcareous clay forms a 1 m thick sediment wedge with clinoforms dipping to the west (subunit 2a, Fig. 3A). To the west this wedge is

replaced by a thinner (0.3 m thick), sheet-like deposit of black organic-rich clay (subunit 2b, Fig. 3C) which merges laterally into palustrine limestone over ~150 m distance. The rooted horizon contains calcrete nodules (Fig. 3B) and a *Assiminea* cf. *aurifera* dominated gastropod fauna with *Cecilioidea* sp., *Lissachatina* cf. *fulica*, *Pseudopeas* sp., *Gulella* sp., *Urocyclidae* indet., and *Pseudoglessula* cf. *boivini*. In subunit 2b (Fig. 3C) gastropods occur more frequently than in subunit 2a and are associated with masses of faecal pellets.

The upper part of the section consists of horizontally bedded palustrine limestone with abundant terrestrial and freshwater gastropods. (unit 3, Fig. 2; Reuter et al., 2009). *Assiminea* cf. *aurifera* is mass occurring. Total thickness of this depositional unit is 10 m (only preserved in the western area of the outcrop (Fig. 3D)).

### Sedimentary evolution

In depositional units 1 and 2 of Mbanja section the smooth, gently sloping surfaces of the argillaceous sediment bodies (Figs. 2 and 3A) point to tidal-flat environments (Dyer, 1998). *Ostreids* (subunit 1a) are characteristic inhabitants of modern tidal flats, where they preferentially colonise the lower regions (Davis and FitzGerald, 2004). Intense rooting in unit 2 documents that duration of tidal flooding decreased, allowing a halophile vegetation to colonise the area.

At modern protected, tropical coasts, the tidal zone is mostly occupied by mangroves extending down to the low tide mark within the lower part of the tidal zone (Davis and FitzGerald, 2004). The fauna in the rooted horizon, however, is transitional between terrestrial and marine. *Assiminea* gastropods are most abundant. Recent *Assiminea* species live in freshwater or slightly brackish water and are common marsh and mangrove dwellers (Vermeij, 1973; Fowler, 1980; Hershler, 1987; Sada, 2001). In contrast, other gastropod taxa occur in much lower numbers. These gastropods are

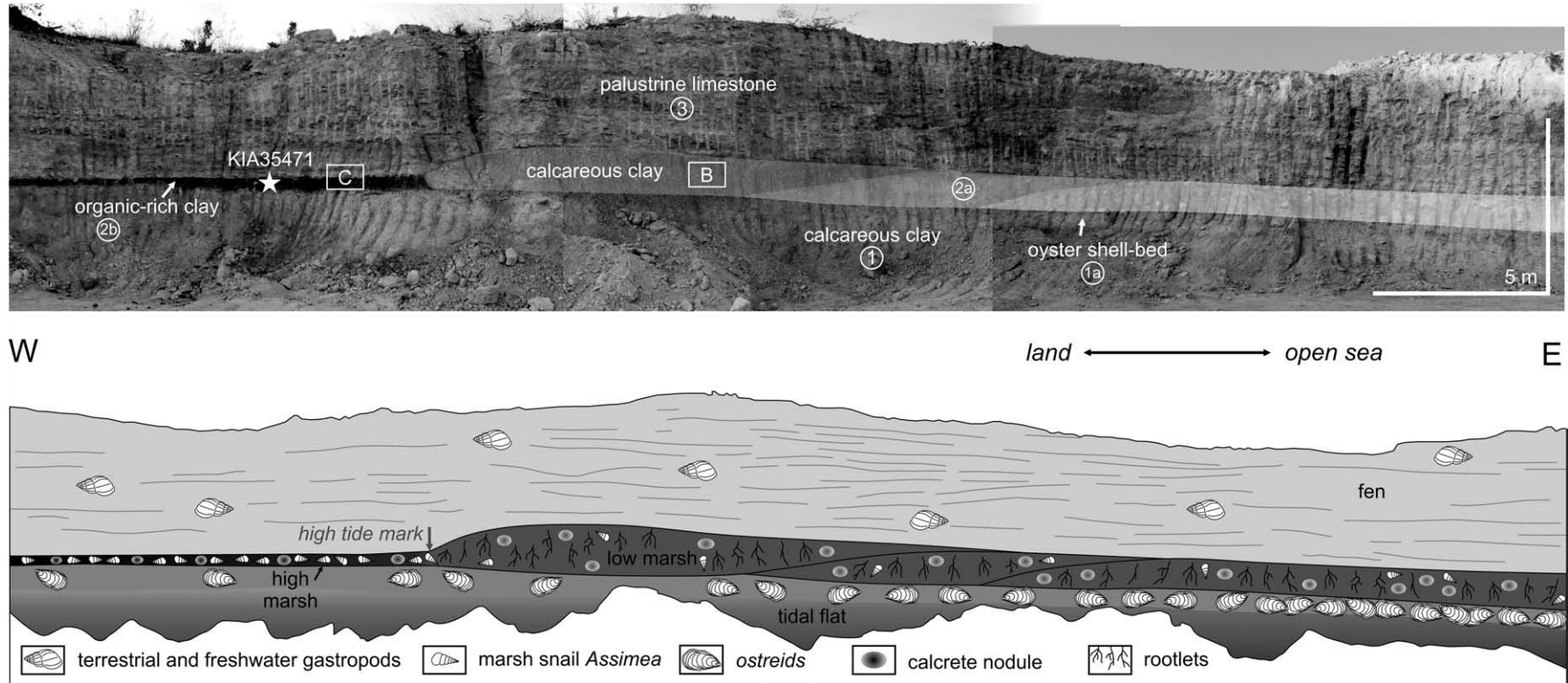


**Figure 2.** Facies architecture and stratal geometries in the studied outcrop at Mbanja. The numbers refer to depositional units described in the text and boxes B and C show the locations of Figures 3B and C. The sampling site of KIA35471 is highlighted by a star. In the eastern part of the quarry (shown in Fig. 2) the palustrine limestone was largely dug. Therefore KIA3572 was sampled in the western part of the quarry (not visible in the Fig. 2) at the top of the palustrine limestone succession.

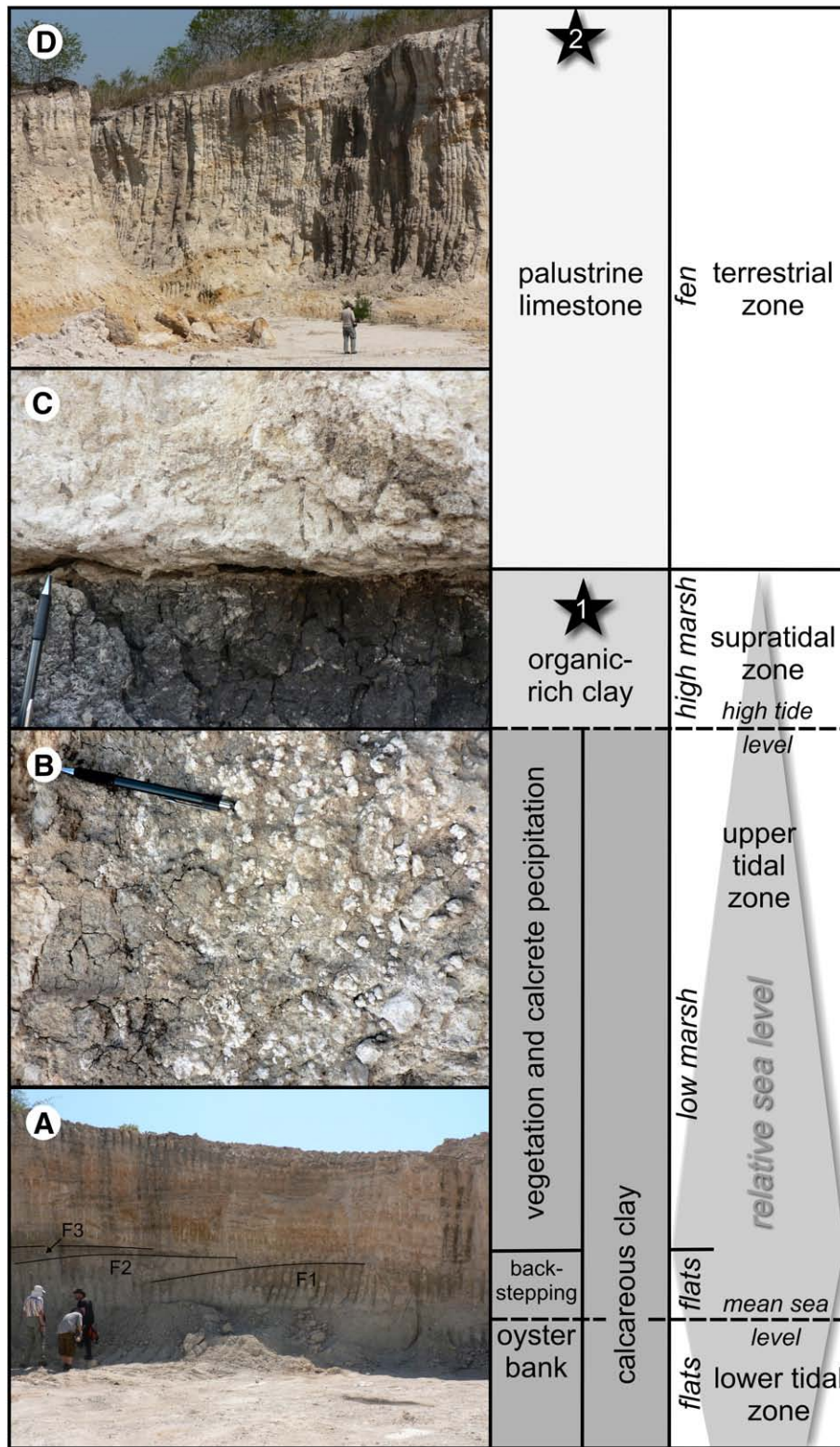


**Figure 3.** Sedimentary cycle in Mbanja outcrop. Stars indicate the stratigraphic position of samples KIA 3571 (1) and KIA3572 (2). (A) Back-stepping of tidal flats in the eastern part of the quarry (F1-3, subunit 2a). (B) Calcrete nodules in calcareous clay from the rooted horizon indicate intensified evaporation in the upper tidal zone (subunit 2a). Length of the pen (for scale): 15 cm. (C) Contact of organic-rich marsh clay (subunit 2b) and palustrine limestone (unit 3). Both facies are intensively penetrated by roots documenting lush vegetation. Length of the pen (for scale): 15 cm. (D) Thick palustrine limestone in the western area of Mbanja quarry (unit 3).

terrestrial and transported from the adjacent mainland; diagnostic mangrove dwellers, as for instance potamidids, are not among them. Mangrove vegetation seems therefore unlikely.

Modern tropical intertidal wetlands that are exposed to longer periods without seawater inundation are prone to strong evaporation

(Ólafsson et al., 2000). These high-salinity areas may be recognised by sparse dwarfed trees and bare patches (Alongi, 1989; Wolanski et al., 1992; Ólafsson et al., 2000). In the studied locality, enhanced evaporation in the higher intertidal zone is documented by calcretes in unit 2 (Fig. 3B) and may be responsible for the absence of

**Table 1**

Radiocarbon dates from southern coastal Tanzania measured at the Leibniz Laboratory for Radiometric Dating and Isotope Research at the Christian-Albrechts-University Kiel (Germany).

Lab. code	Site	Stratigraphic position in the outcrop	Sample description	Conventional radiocarbon date ( $^{14}\text{C}$ yr BP)
KIA35471	Mbanja quarry (09°53.34'S, 39°43.37'E)	Organic-rich clay (subunit 2b)	<i>Assiminea</i> shell (aragonite)	43,983 + 1907/– 1540
KIA35472	Mbanja quarry (09°53.34'S, 39°43.37'E)	Palustrine limestone (top unit 3)	<i>Assiminea</i> shell (aragonite)	33,112 + 487/– 459

mangroves. In those areas of modern intertidal zones where harsh growing conditions exclude mangroves and other tall plants, salt marshes occupy the upper tidal zone above mean sea level, where they receive regular but infrequent tidal flooding.

The net deposition in modern marshes was observed to increase with the number of tidal inundations and therefore the greatest deposition occurs just below the limit of high tides (Brown, 1998). The transition from calcareous clay (subunit 2a) to organic-rich clay (subunit 2b) corresponds with a distinct change in thickness (Fig. 2). It is accompanied by a drastic increase of *Assiminea* shells. These gradients reflect decreasing marine influence in a western direction and are consistent with the east–west transition from tidal (units 1 and 2) to terrestrial facies (unit 3). Therefore, we interpreted the change from subunit 2a to subunit 2b to represent the high tide level (Figs. 2 and 3).

The palustrine limestone (unit 3, Fig. 2) was precipitated within microbial mats in a seasonally, barely flooded grassland, which was comparable to the present-day Floridian Everglades marl prairies (Reuter et al., 2009).

### Stratigraphy

The boundary surface between units 2 and 3 marks the transition from marginal marine to terrestrial facies (Figs. 2 and 3). Measurements with an altimeter calibrated to sea level document a 21 m altitude difference between this surface and present-day sea level. Correlated with the terrace stratigraphy for northern Tanzania this height fits the intra-Weichselian Tanga Terrace, which is elevated 20–40 m above present-day sea level (Alexander, 1968).

For age determination we used shells of the marsh snail *Assiminea* from the organic-rich clay subunit 2b (sample KIA35471) and from top of the palustrine limestone unit 3 (sample KIA35472) for radiocarbon dating (Fig. 3). *Assiminea* was chosen because it is a semi-aquatic minute snail. Compared to other terrestrial gastropods, this group can provide reliable  $^{14}\text{C}$  ages because they incorporate only small amounts of 'old' carbon depleted in  $^{14}\text{C}$  (Brennan and Quade, 1997).

Before analysis, gastropod shells were cracked and shell fragments screened under SEM and optical microscope to detect any diagenetic alteration and contamination. AMS  $^{14}\text{C}$  measurements were performed at the Leibniz Laboratory for Radiometric Dating and Isotope Research at the Christian-Albrechts-University Kiel (Germany) with a 3 MV Tandem AMS. The uncalibrated radiocarbon ages indicate a Weichselian age for the *Assiminea* shells from the organic-rich clay (43,983 + 1907/– 1540  $^{14}\text{C}$  yr BP) as well as from the palustrine limestone (33,112 + 487/– 459  $^{14}\text{C}$  yr BP; Table 1). Because the obtained ages are close to the limit of AMS technique (45 ka) they could be interpreted as infinite ages if contaminated with modern carbon. Radiocarbon ages are quoted with one standard deviation (s.d.) only, which means that there is only 68% certainty that the true age falls within these limits.  $2 \times \text{s.d.}$  gives 95% confidence (Bowman, 1990). Considering an approximate normal distribution and standard deviation of + 1.9  $^{14}\text{C}$  ka the age of sample KIA35471 is <48  $^{14}\text{C}$  ka BP with 95% confidence. In contrast, the age of sample KIA35472 is 100% <45 ka at  $2 \times \text{s.d.}$  and therefore probably finite. We think the 44.0 + 1.9/– 1.5  $^{14}\text{C}$  ka BP date of sample KIA35471 is also finite because both ages are >30 ka and KIA35472, which has the younger age, was sampled stratigraphically higher in the outcrop (Table 1). Because  $^{14}\text{C}$  calibration of terrestrial systems is limited to 1175  $^{14}\text{C}$  yr BP in the southern hemisphere (McCormac et al., 2004) calibration of the "raw" radiocarbon ages is not possible.

### Emergence of the Lindi coast

#### Effects of global ice volume build-up during the last glaciation

The reconstructed coastal wetland formed prior to the global last glacial maximum during a phase of long-term ice build-up and falling sea level. Fine-scale climate fluctuations, which produced high-frequency, low-amplitude sea-level changes, were superimposed on this long-term climate trend (Fig. 4). Taking the  $2 \times \text{s.d.}$  of the 44.0 + 1.9/– 1.5  $^{14}\text{C}$  ka BP age for sample KIA35471 (48–41  $^{14}\text{C}$  ka BP) into account, the back-stepping of tidal flats in unit 2 (Figs. 2 and 3A)

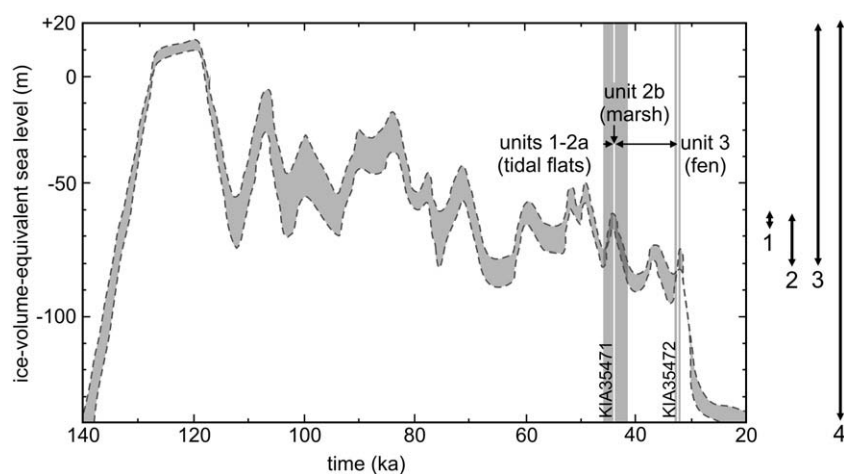


**Figure 4.** Diagram illustrating the relationships between facies evolution, ice-volume-equivalent sea level (modified from Lambeck and Chapell, 2001; the confidence interval is indicated by dashed lines), and tectonic uplift between the last two glacial maxima at about 140 ka and 20 ka. (1) Sea level at 44  $^{14}\text{C}$  ka BP. (2) Sea level at 44.0 + 1.9/– 1.5  $^{14}\text{C}$  ka BP. (3) Altitude difference of the sea level between 44.0 + 1.9/– 1.5  $^{14}\text{C}$  ka BP and the present day at the outcrop. (4) Altitude difference of the sea level between 20 ka and the present day at the outcrop.

reflects a rising sea level during the small-scale transgression in the 46–44 <sup>14</sup>C ka BP interval (Fig. 4). At ~44 <sup>14</sup>C ka BP, when the organic-rich clay of unit 2 was deposited, the speed of sea-level rise decreased (Fig. 4). At this stage, sediment supply was strong enough to fill up the accommodation space and enabled development of intertidal vegetation. The subsequently installed fen continued until ~33 <sup>14</sup>C ka BP. This date corresponds with the onset of the Last Glacial Aridity Maximum in equatorial East Africa which lasted from 32 to 14 ka (McGlue et al., 2007). The wetland dried up at this time (Reuter et al., 2009).

Because the <sup>14</sup>C ages of KIA35471 and KIA35472 are not calibrated they cannot be placed precisely on the time line in Figure 4. However, the reconstructed depositional history of the coastal terrace is demonstratively consistent with the ice-volume-equivalent sea-level curve of Lambeck and Chapell (2001) when using the <sup>14</sup>C ages as pinning points (Fig. 4). Thus we decided it is justified to plot the “raw” radiocarbon ages on the time line shown in Figure 4 to estimate the effects of sea level and tectonics for the emergence of the Lindi coast.

#### Effects of extensional tectonics in the East African Rift System

At 44.0 ± 1.9/–1.5 <sup>14</sup>C ka BP the eustatic sea level was 60–90 m below present-day sea level (Lambeck and Chapell, 2001; Fig. 4). Therefore, the position of the studied coastal terrace at ~21 m above present-day sea level cannot refer to eustatic sea-level fluctuations. Consistent with these observations, the post-sedimentary inverse fault striking parallel to the LFZ observed west of the studied outcrop, documents tectonic activity at the LFZ after ~33 <sup>14</sup>C ka BP.

Since ~44 <sup>14</sup>C ka BP the terrace was elevated 80–90 m (1.8–2.0 mm/yr) as indicated by the 44 <sup>14</sup>C ka BP date, or 80–110 m (1.8–2.5 mm/yr) if confidence interval of +1.9/–1.5 <sup>14</sup>C ka is considered (Fig. 4). Comparable uplift magnitudes have been estimated for the rift flanks of the EARS during the Plio-Pleistocene. The >5000 m high Rwenzori Mountains (Uganda, Fig. 1) and adjacent rift flanks represent one of the most extreme examples of rift-mountain uplift on earth (Ring, 2008). MacPhee (2006) reported an average minimum uplift rate of 1600 m/Ma for the last 2.5 Ma in the Rwenzoris. This equates to 70 m uplift in 44 ka (1.6 mm/yr), what is slightly lower than our findings. However, the data was potentially biased by the long averaging interval and non-steady Rwenzori uplift (MacPhee, 2006; Ring, 2008). Major uplift was recognized since the onset of Rwenzori glaciation during the middle Pleistocene when glacial erosion and glacier retreat during interglacial periods promoted uplift through isostatic rebound (Ring, 2008).

Assuming that a transpressive tectonic regime at Lindi coast occurred not before ~33 <sup>14</sup>C ka BP, as indicated by a post-sedimentary reverse fault in the study area, the late Quaternary uplift at the Lindi coast must have been even higher than 1.8–2.5 mm/yr. For the late Weichselian, Ring (1994) demonstrated localised uplift of rift blocks in the Malawi Rift, at the western boundary of the Rovuma Plate (Stamps et al., 2008; Fig. 1), which deformed the 20 ka and younger Chitimwe Beds and occurred along restraining bends of strike-slip faults. Le Gall et al. (2004) argued for a structural link of the Malawi Rift with the eastern rift branch via the Kilombero Rift and Maminzi Transverse Fault Zone (Fig. 1) during the Quaternary and Stamps et al. (2008) showed that localised strain along narrow rift structures that isolate large lithospheric blocks as the Rovuma Microplate was due to rifting in the EARS. Therefore, deformation of the Chitimwe Beds might be linked to shifting of the Rovuma Microplate even though the Malawi Rift is part of the western rift branch. If reactivation of the LFZ occurred contemporaneously with deformation of the Chitimwe Beds since 20 ka, uplift of the Lindi coast would have been 8.0 mm/yr. This is 5 times higher than in the Rwenzoris and therefore considered as a highly unrealistic value—particularly there was no isostatic rebound through ice melting and glacial erosion at the East African coast. Therefore we suggest that tectonic uplift in southern coastal Tanzania

was already in progress prior to the last glaciation maximum and accelerated the exposure of the studied coastal terrace at 44.0 ± 1.9/–1.5 <sup>14</sup>C ka BP. Interestingly, along the northern segment of the western branch of the EARS a distinct phase of volcanic activity occurred at ~50 ka and initiated a phase of continuing rifting (Boven et al., 1998; Lærdal and Talbot, 2002).

#### Conclusions

Weichselian sediments in southern coastal Tanzania revealed a transition from tidal flats to a fen. This succession documents a falling relative sea level. Based on radiocarbon dating of *Assimea* shells we show that emergence of the coastal terrace between Lindi Bay and Mchinga Bay occurred prior to the last glaciation maximum through the coincidence of eustatic sea level fall and tectonic uplift at the LFZ. At ~44 <sup>14</sup>C ka BP the coast was exposed above sea level and a coastal wetland evolved. Since that time, vertical displacement was in the range of 80–110 m. Results show that late Quaternary, rift-related, vertical plate movements at the Tanzanian coast have been of similar magnitude as in the Rwenzori Mountains in the EARS.

#### Acknowledgments

We appreciate the reviews of two anonymous referees and the critical editorial advice of J. U. Fucugauchi (Mexico City) and A. Gillespie (Seattle). Funding by the FWF (grant P18189) is gratefully acknowledged.

#### References

- Alexander, C.S., 1968. The marine terraces of the northeast coast of Tanzania. *Zeitschrift für Geomorphologie Neue Folge Supplement* 7, 133–154.
- Alongi, D.M., 1989. The role of soft-bottom benthic communities in tropical mangrove and coral reef ecosystems. *Reviews in Aquatic Sciences* 1, 243–279.
- Arthurton, R., 2003. The fringing reef coasts of eastern Africa—present processes in their long-term context. *Western Indian Ocean Journal of Marine Sciences* 2, 1–13.
- Arthurton, R.S., Brampton, A.H., Kaaya, C.Z., Mohamed, S.K., 1999. Late Quaternary coastal stratigraphy on a platform fringed tropical coast—a case study from Zanzibar, Tanzania. *Journal of Coastal Research* 15, 635–644.
- Boven, A., Pasteels, P., Punzalan, L.E., Yamba, T.K., Musisi, J.H., 1998. Quaternary perpotassic magmatism in Uganda (Toro-Ankole Volcanic Province): age assessment and significance for magmatic evolution along the East African Rift. *Journal of African Earth Sciences* 26, 463–476.
- Bowman, S., 1990. *Radiocarbon Dating*. British Museum Press, London.
- Braithwaite, C.J.R., 1984. Depositional history of late Pleistocene limestones of the Kenya coast. *Journal of the Geological Society, London* 141, 685–699.
- Brennan, R., Quade, J., 1997. Reliable late-Pleistocene stratigraphic ages and shorter groundwater travel times from <sup>14</sup>C in fossil snails from the southern Great Basin. *Quaternary Research* 47, 329–336.
- Brown, S.L., 1998. Sedimentation on a Humber saltmarsh. In: Black, K.S., Paterson, D.M., Cramp, A. (Eds.), *Sedimentary Processes in the Intertidal Zone*, 139. Geological Society of London, Special Publications, pp. 69–83.
- Calais, E., Hartnady, C., Ebinger, C., Nocquet, J.M., 2006. Kinematics of the East African Rift from GPS and earthquake slip vector data. In: Yiru, G., Ebinger, C.J., Maguire, P.K.H. (Eds.), *Structure and Evolution of the Rift Systems within the Afar Volcanic Province, Northeast Africa*, 259. Geological Society of London, Special Publications, pp. 9–22.
- Davis, R.A., FitzGerald, D.M., 2004. *Beaches and Coasts*. Blackwell, Oxford.
- Dyer, K.R., 1998. The typology of intertidal mudflats. In: Black, K.S., Paterson, D.M., Cramp, A. (Eds.), *Sedimentary Processes in the Intertidal Zone*, 139. Geological Society of London, Special Publications, pp. 11–24.
- Forster, A., Ebinger, C., Mbede, E., Rex, D., 1997. Tectonic development of the northern Tanzanian sector of the East African Rift System. *Journal of the Geological Society, London* 154, 689–700.
- Fowler, B.H., 1980. Reproductive biology of *Assimea californica* (Tyron, 1865) (Mesogastropoda: Rissoacea). *Veliger* 23, 163–166.
- Hershler, R., 1987. Redescription of *Assimea infima* Berry, 1947 from Death Valley, California. *Veliger* 29, 274–288.
- Kent, P.E., Hunt, J.A., Johnstone, D.W., 1971. *The geology and geophysics of coastal Tanzania*. Institute of Geological Sciences, HMs Stationary Office London, Geophysical Paper, p. 6.
- Lambeck, K., Chapell, J., 2001. Sea level change through the last glacial cycle. *Science* 292, 679–686.
- Le Gall, B., Rolet, J., Ebinger, C., Gloaguen, R., Nilsen, O., Dypvik, H., Deffontaines, B., Mruma, A., 2004. Neogene-Holocene rift propagation in central Tanzania: morphostructural and aeromagnetic evidence from the Kilombero area. *Geological Society of America Bulletin* 116, 490–510.

- Lærdal, T., Talbot, M.R., 2002. Basin neotectonics of Lakes Edward and George, East African Rift. *Palaeogeography, Palaeoclimatology, Palaeoecology* 187, 213–232.
- McCormac, G., Hogg, A.G., Blackwell, P.G., Buck, C.E., Higham, T.F.G., Reimer, P.J., 2004. SHCal04 southern hemisphere calibration, 0–11.0 cal kyr BP. *Radiocarbon* 46, 1087–1092.
- McGlue, M.M., Lezzar, K.E., Cohen, A.S., Russell, M., Tiercelin, J.J., Felton, A.A., Mbede, E., Nkotagu, H.H., 2007. Seismic records of late Pleistocene aridity in Lake Tanganyika, tropical East Africa. *Journal of Paleolimnology* 40, 635–653.
- MacPhee, D., 2006. Exhumation, rift-flank uplift, and the thermal evolution of the Rwenzori Mountains determined by combined (U-Th)/He and U-Pb thermochronometry. Massachusetts Institute of Technology, unpublished PhD-thesis.
- Mougenot, D., Recq, M., Virlogeux, P., Lepvrier, C., 1986. Seaward extension of the East African Rift. *Nature* 321, 599–603.
- Nicholas, C.J., Pearson, P.N., McMillan, I.K., Ditchfield, P.W., Singano, J.M., 2007. Structural evolution of southern coastal Tanzania since the Jurassic. *Journal of African Earth Sciences* 48, 273–297.
- Ólafsson, E., Carlström, S., Ndaro, S.G.M., 2000. Meiobenthos of hypersaline tropical mangrove sediment in relation to spring tide inundation. *Hydrobiologia* 426, 57–64.
- Rabinowitz, P.D., Coffin, M.F., Falvey, D.A., 1983. The separation of Madagascar and Africa. *Science* 220, 67–69.
- Reuter, M., Piller, W.E., Harzhauser, M., Kroh, A., Berning, B., 2009. A fossil Everglades-type marl prairie and its paleoenvironmental significance. *Palaios* 24, 747–755.
- Ring, U., 1994. The influence of preexisting structure on the evolution of the Cenozoic Malawi rift (East African Rift System). *Tectonics* 13, 313–326.
- Ring, U., 2008. Extreme uplift of the Rwenzori Mountains in the East African Rift, Uganda: Structural framework and possible role of glaciations. *Tectonics* 27, TC4018.
- Ring, U., Schwartz, H., Bromage, T.G., Sanaane, C., 2005. Kinematic and sedimentologic evolution of the Manyara Rift in northern Tanzania, East Africa. *Geological Magazine* 142, 355–368.
- Sada, D.W., 2001. Demography and habitat use of the badwater snail (*Assiminea infima*), with observations on its conservation status, Death Valley National Park, California, U.S.A. *Hydrobiologia* 466, 255–265.
- Schlüter, T., 1997. *Geology of East Africa*. Gebrüder Bornträger, Berlin–Stuttgart.
- Shaghude, Y.W., Wannäs, K.O., 2000. Mineralogical and biogenic composition of Zanzibar channel sediments, Tanzania. *Journal of Estuarine Coast and Shelf Sciences* 51, 477–489.
- Stamps, S.D., Calais, E., Saria, E., Hartnady, C., Nocquet, J.M., Ebinger, C.J., Fernandes, R.M., 2008. A kinematic model for the East African Rift. *Geophysical Research Letters* 35, L05304.
- Vermeij, G.J., 1973. Molluscs in mangrove swamps: physiognomy, diversity, and regional differences. *Systematic Zoology* 22, 609–624.
- Wolanski, E., Mazda, Y., Ridd, P., 1992. Mangrove hydrodynamics. In: Robertson, A.I., Alongi, D.S. (Eds.), *Tropical Mangrove Ecosystems*. American Geophysical Union, Washington D.C., pp. 43–62.